# Direct Power and Torque Control of AC/DC/AC Converter with Induction Generator for Renewable Energy System – Wave Dragon MW

MAREK JASINSKI, MARIAN P. KAZMIERKOWSKI
Electrical Department Institute of Control and Industrial Electronics
Warsaw University of Technology
ul. Koszykowa 75, 00-662 Warsaw
POLAND
http://www.isep.pw.edu.pl

*Abstract:* - In the paper a Direct Power and Torque Control-Space Vector Modulated (DPTC-SVM) are presented. This strategy leads to good dynamic and static behaviors. Additional power feedforward (PF) loop from a generator side converter (GSC) to line side converter (LSC) control improves dynamic of the power flow. As a result, more accurate input-output energy matching allows better stabilization of DC-link voltage. Hence, life time of DC-link capacitors would be prolongated. Moreover, proposed advanced control strategy gives possibility of control in whole power range of active and reactive rated power injected to the line. Current delivered to the line is sinusoidal like in shape (THD < 5 %). Presented system is considered to be implemented in wave energy converter – Wave Dragon MW [1].

*Key-Words:* - Power Electronics in Renewable Energy, Wave Dragon MW, Direct Power and Torque Control

## 1 Introduction

Well controlled power electronics interface for renewable energy system can improve a quality of a “clean power” from renewable sources such as sea waves [1]. One example from many possibilities is presented in the paper.

Applied AC/DC/AC converter allows controlling energy at the generator side separately from line side. DC-link takes a role of a buffer between line and generator. However, voltage fluctuations in DC-link can have a negative impact on life time of the dc capacitors and line power quality. The capacitors have some main drawbacks: low reliability, big size, weight and cost. Hence, reliability of the DC-link capacitor is the major factor limiting the life time of the power electronics converter systems. DC voltage stabilization at desired level can extend life time of capacitors because overvoltage usually causes capacitors breakdown.

Development of control methods for Pulse Width Modulated (PWM) line side converter (LSC) was possible thanks to advances in power semiconductors devices and Digital Signal Processors (DSP). Therefore, the Insulated Gate Bipolar Transistors (IGBT) AC/DC/AC converter controlled by PWM is used in power electronics systems (Fig.1). Thanks to controlled LSC the DC-link voltage fluctuation can be reduced. Farther reduction of the DC-link voltage fluctuation can be achieved by active power feedforward loop from generator side to the control of the LSC [3].

In respect to line power quality and dc-voltage stabilization power balance between line and generator is very important. Therefore, to improve instantaneous input/output power matching, the additional active power feedforward (PF) control loop is introduced. Its deliver information about gen. state directly to active power control loop of the LSC.

Thanks to better control of the power flow the fluctuation of the DC-link voltages will be decreased. Moreover, active and reactive power control ability in a whole range of generator power allows improving system efficiency and quality of an energy delivered to the line.

Therefore, well designed control methods (estimators, controllers’ parameters in control loops etc.) for line side converter (LSC) as well as for generator side converter (GSC) have a major impact on main parameter of the renewable energy system.

## 2 Renewable energy system Wave Dragon – MW [4]

Needs for the development of renewable energy, including offshore wave energy, arises from the requirement to strengthen the security of supply, reduce emissions of greenhouse and acid rain gases. As an example the UK Government has a target of generating 10% of UK electricity demand from renewable sources by 2010, 15% by 2015 with an aspiration of 20% by 2020. The Wave Dragon MW (Fig.2) is an offshore wave energy converter (WEC) of the overtopping type. The development work is to a large extent built on the concept: use proven technologies when going offshore. The plant consists of two wave reflectors focusing the incoming waves towards a ramp, a reservoir for collecting the overtopping water and a number of hydro turbines for converting the pressure head into mechanical power. Generators connected with turbines convert mechanical into

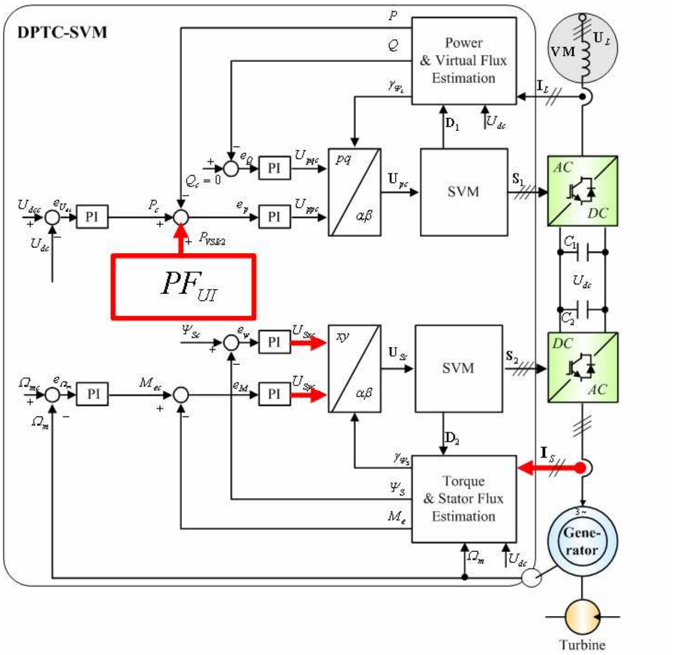


Fig. 1 Structure of Direct Power and Torque Control-Space Vector Modulated (DPTC- SVM) with active power feedforward (PF)
Where: VM- virtual machine, SVM- space vector modulator, PF – active power feedforward

electrical power which is controlled by power electronics AC/DC/AC converters. Wave Dragon is the largest known wave energy converter today [4]. Each unit will have a rated power of 4-11 MW or more depending on how energetic the wave climate is at the deployment site. The utilization of the overtopping principle as opposed to power absorption via moving bodies means that the efficiency grows with the size of the converter. This means that only practical matters set limits for the size of this WEC. In addition to this Wave Dragon due to its large size can act as a floating foundation for MW wind turbines, thus adding a very significant contribution to annual power production at a marginal cost. This boost in profitability makes Wave Dragon an economical profitable investment with the prices for renewable electricity.

Wave Dragon (WD) has been developed during the last nine years. Grid connected prototype presented in Fig. 3 (a scale 1:4.5 of a North Sea production plant) of the WD MW is presently being tested in a Danish fjord Nissum Bredning. Every activity is focused on one goal: to produce electricity with the highest efficiency in the lowest possible costs – and in an environmental friendly and reliable way.

The only way to achieved this goal (from power electronics point of view) is choosing proper generating system and power electronics converter with robust and accuracy control methodology.

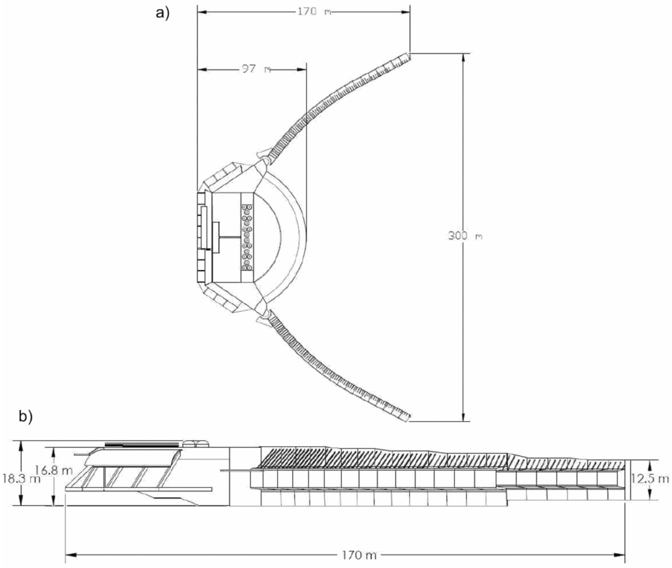


Fig. 2 Top view of the Wave Dragon MW a); Side view of the Wave Dragon MW b) [4]

## 3 Direct Power and Torque Control of AC/DC/AC Converter with Induction Generator

Base on literature analysis very promising for control of an AC/DC/AC converter are direct power control with space vector modulation (DPC-SVM) and direct torque control with space vector modulation (DTC-SVM). When both methods are joined for control of the AC/DC/AC converter connected between electrical machine and supply line direct power and torque control with space vector modulation is obtained – DPTC-SVM [3].

### 3.1 Direct Torque Control with Space Vector Modulation – DTC-SVM

To avoid the drawbacks of switching table based DTC [5] instead of hysteresis controllers and switching table the PI controllers with the SVM block were introduced like in field oriented control (FOC). Therefore, DTC-SVM joins DTC and FOC features in one control structure as in Fig. 1.


Fig. 3 Prototype of Wave Dragon in fjord Nissum Bredning [1]

For needs of the DTC-SVM method a mathematical model of machine in a xy rotating system of coordinates are chosen ($\Omega_K = \Omega_{\Psi_S}$ ). In this case the coordinate system is oriented with $x$ stator flux linkage component. The command electromagnetic torque $M_{ec}$ is delivered from outer PI speed controller (Fig. 1). Then, $M_{ec}$ and command stator flux $\Psi_{Sc}$ amplitudes are compared with estimated actual values of $M_e$ and $\Psi_S$. The torque $e_M$ and flux $e_\psi$ errors are fed to two PI controllers. The output signals are the command stator voltage components $U_{Syc}$, and $U_{Sxc}$ respectively.

Further, voltage components in rotating $xy$ system of coordinates are transformed into $\alpha\beta$ stationary coordinates using $\gamma_{\Psi_S}$ flux position angle. Obtained voltage vector $\mathbf{U}_{Sc}$ is delivered to SVM which generates appropriate switching states vector $\mathbf{S}_2(S_{2A}, S_{2B}, S_{2C})$ for the GSC. An exhausting description of the DTC-SVM can be found in [6].

## 3.2 Direct Power Control with Space Vector Modulation – DPC-SVM

Direct power control with space vector modulation – DPC-SVM guarantees high dynamics and static performance via an internal power control loops. It is not well known in the literature. This method joins the concept of DPC and virtual flux (VF) oriented control (V-FOC). The active and reactive power is used as control variables instead of the line currents.

The DPC-SVM with constant switching frequency uses closed active and reactive power control loops (Fig. 1). The command active power $P_c$ are generated by outer DC-link voltage controller, whereas command reactive power $Q_c$ is set to zero for unity power factor operation. These values are compared with the estimated $P$ and $Q$ values respectively. Calculated errors $e_p$ and $e_Q$ are delivered to PI power controllers. Voltages generated by power controllers are DC quantities, what eliminates steady state error (PI controllers features). Then after transformation to stationary $\alpha\beta$ coordinates using $\gamma_{\Psi_L}$ VF position angle, the voltages are used for switching signals generation by SVM block. The proper design of the power controller parameters is very important especially in respect to line side power quality. Therefore, analysis and synthesis will be described in the followed Subsection.

### 3.2.1 Line Side Power Controllers

The assumptions are described in detail in [3]. A block diagram for a simplified power control loop in the synchronous $xy$ rotating coordinates is presented. Since, the same block diagram applies to both $P$ and $Q$ power controllers, description only for $P$ active power control loop

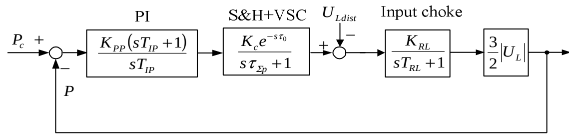


Fig. 4 Block diagram for a simplified active power control loop in the synchronous rotating reference frame

will be presented. Control structure will operates in discontinuous environment (model in Saber, and implementation in DSP) therefore, is necessary to take into account the sampling period $T_S$. It could be done by sample & hold – S&H block. Moreover, the statistical delay of the PWM generation $T_{PWM} = 0.5T_S$ should be taken into account (voltage source converter (VSC) block). In the literature the delay of the PWM is approximated from zero to two sampling periods $T_S$. Further, $K_C = 1$ is the VSC gain, $\tau_0$ is a dead time of the VSC ($\tau_0 = 0$ for ideal converter). The S&H and VSC blocks could be joined in one S&H+VSC block. Where, sum of their time constants is expressed by:

$$\tau_{\Sigma p} = T_S + T_{PWM} \tag{1}$$

Please note that, $\tau_{\Sigma p}$ is a sum of small time constants, $T_{RL} = L/R$ is a large time constant and $K_{RL} = 1/R$ is a gain of input choke. Hence, $T_{RL}$ gives a dominant pole. Between several methods of analysis, there are two simple way for the controller parameters design: modulus optimum - MO and symmetry optimum – SO. Tuning of the regulators based on and MO gives good response to a step change of reference (4% overshoot). But an answer for a step of a disturbance signal is not satisfactory (about $3T_{RL}$) whereas, the SO has much better capabilities in transient for disturbance signal step ($U_{Ldist}$ e.g. higher harmonics, voltage flicker etc.). Therefore, it is better to choice the SO for further consideration.

For constant line voltage $U_L = const.$ the following open loop transfer function can be derived:

$$G_{OP}(s) = \frac{K_{RL}K_{PP}(1+sT_{IP})}{sT_{IP}(s\tau_{\Sigma p}+1)(sT_{RL}+1)}\frac{3}{2}|U_L| \tag{2}$$

With simplification $(sT_{RL}+1) \approx sT_{RL}$ gives following closed loop transfer function for power control loop:

$$G_{ZP}(s) = \frac{K_{RL}K_{PP}(1+sT_{IP})}{K_{RL}K_{PP}(1+sT_{IP}) + s^2T_{IP}T_{RL} + s^3T_{IP}\tau_{\Sigma p}T_{RL}}\frac{3}{2}|U_L| \tag{3}$$

For this relation the proportional gain and integral time constant of the PI current controller can be calculated as:

$$K_{PP} = \frac{T_{RL}}{2\tau_{\Sigma p}K_{RL}}\frac{2}{3|U_L|} \tag{4}$$

$$T_{IP} = 4\tau_{\Sigma p} \tag{5}$$

which, substituted in Eq. (2), yields open loop transfer function of the form:

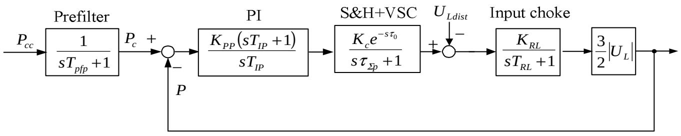


Fig. 5 Power control loop with prefilter

$$G_{OP}(s)=\frac{2T_{RL}}{2\tau_{\Sigma p}K_{RL}3|U_L|}\frac{K_{RL}(1+s4\tau_p)}{s4\tau_{\Sigma p}(s\tau_{\Sigma p}+1)(sT_{RL}+1)}\frac{3}{2}|U_L| \approx \frac{T_{RL}}{2\tau_{\Sigma i}}\frac{(1+s4\tau_{\Sigma p})}{s4\tau_{\Sigma p}(s\tau_{\Sigma p}+1)sT_{RL}}=\frac{(1+s4\tau_{\Sigma p})}{s^2 8\tau_{\Sigma p}^2+s^3 8\tau_{\Sigma p}^3}. \tag{6}$$

For the closed loop transfer function:

$$G_{CP}(s)=\frac{1+s4\tau_{\Sigma p}}{1+s4\tau_{\Sigma p}+s^2 8\tau_{\Sigma p}^2+s^3 8\tau_{\Sigma p}^3}. \tag{7}$$

Tuning of the regulators based on Eqs. (4) and (5) gives power tracking performance with more then 40% overshoot as shown in Fig. 6a and Fig. 7a caused by the forcing element in the numerator (Eq. (7)). Therefore, for decreasing the overshot (compensate for the forcing element in the numerator) a first order prefilter on the reference signal can be used:

$$G_{pfp}(s)=\frac{1}{1+sT_{pfp}} \tag{8}$$

Where, $T_{pfp}$ usually equals to a few $\tau_{\Sigma p}$. Hence, the block diagram of the control loop takes a form as in Fig. 5.
In further investigation a time delay of the prefilter is set to $4\tau_{\Sigma p}$. So that Eq. (7) takes a form:

$$G_{CPf}(s)=G_{CP}(s)G_{pfp}(s)=\frac{1}{1+s4\tau_{\Sigma p}+s^2 8\tau_{\Sigma p}^2+s^3 8\tau_{\Sigma p}^3}. \tag{9}$$

Discrete simulations (fs=5kHz) in Fig. 7 show that the answer is little bit different in comparison with continuous simulation in Fig. 6. The difference is caused because of presence of the nonlinear coupling (discrete simulation was made with modeled coupling). Finally the relation (9) can be approximated by first order transfer function (results in Fig. 6):

$$G_{Cpf}(s)\cong\frac{1}{1+s4\tau_{\Sigma p}}=\frac{1}{1+sT_{IT}}. \tag{10}$$

For better comparison with experimental results, the test under distorted line voltage was performed. Command power has been changed from 1kW to 2.5 kW. The simulation result for this case is shown in Fig. 8.
Please take into account the oscillations in Fig. 8. There are

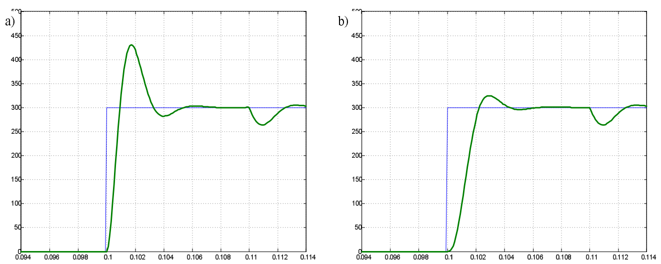

Fig. 6 Active power tracking performance (simulated in Matlab Simulink) controller parameters designed according to SO; a) without prefilter, b) with prefilter

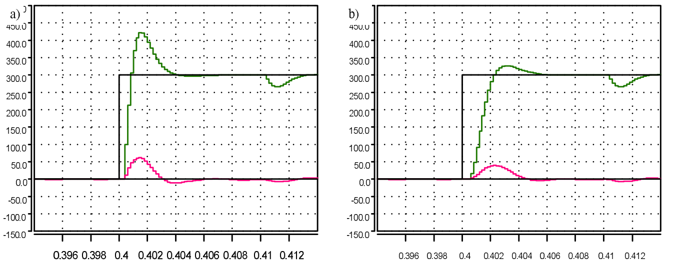

Fig. 7 Active power tracking performance (simulated in Saber) without decoupling; a) without prefilter, b) with prefilter
From the top: command and estimated active power, command and estimated reactive power

generated by modeled line voltage distortion ($THD_{U_L}$ = 4 % of 5-th harmonics). This harmonics after coordinate transformation to rotating coordinates gives AC components with frequency six times higher then line voltage frequency. Hence, the question is appearing: how the sampling frequency takes impact on the line side power control parameters, and on the design of the power controllers? Therefore, please take into consideration the following simulated results presented in Fig. 9. It shows active and reactive power tracking performance at different sampling frequency: fs=10kHz (a,b), and fs=20kHz (c,d).

### 3.3 Active power feedforward – PF

In spite of very good dynamics behaviors of DPTC-SVM scheme, the control of the DC-link voltage can be improved. Therefore, active power feedforward – PF from generator side converter (GSC) to line side converter (LSC) was introduced. The PF deliver information about machine states directly to active power control loop of the LSC. Thanks to faster control of power flow between generator and line, the fluctuation of the DC-link voltages will be significantly decreased. So, the life time of the DC-link capacitors should be extended. In Fig. 10 is shown simplified diagram of the AC/DC/AC converter which consist of LSC and GSC. Both converters are IGBT bridge converter.

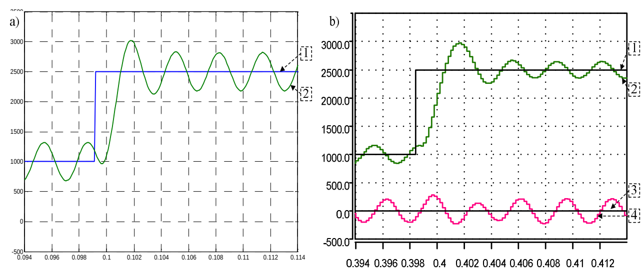

Fig. 8 Active power tracking performance (simulated) with prefilter; 1) command active power, 2) estimated active power, 3) command reactive power, 4) estimated reactive power; a) simulation in Matlab Simulink b) simulation in Saber fs=5kHz

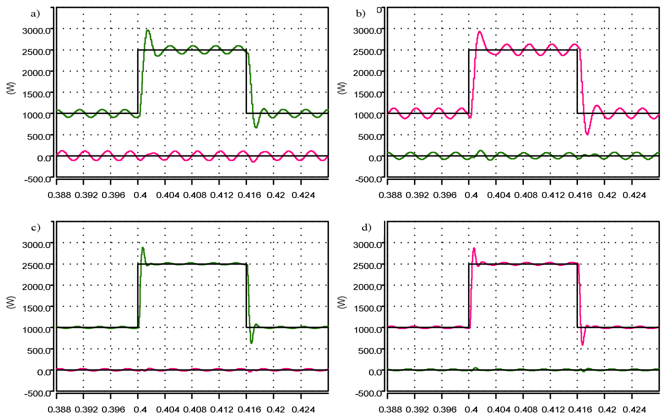


Fig. 9 Active and reactive power tracking performance (simulated in Saber) at different sampling frequency: fs=10kHz a) active power step, and b) reactive power step; fs=20kHz c) active power step and d) reactive power step

From the top: (a,c) command and estimated active power, command and estimated reactive power, (b,d) command and estimated reactive power, command and estimated active power

Note again that, the coordinates system for control of the LSC is oriented with VF vector. Therefore, $I_{Lxc}$ is set to zero to meet the unity power factor (UPF) condition. With this assumption the line side power of LSC can be calculated as:

$$P_{LSC} = \frac{3}{2}\left(I_{Lx}U_{px} + I_{Ly}U_{py}\right) = \frac{3}{2}I_{Ly}U_{py} \qquad (11)$$

Under steady states operation $I_{Ly} = const.$ and, with assumption that resistance of the input choke is $R = 0$, the following equation can be written:

$$P_{LSC} = \frac{3}{2}I_{Ly}U_{Ly} \qquad (12)$$

Another form of the above equations can be derived based on VF where is clearly seen that the active power of the LSC is proportional to the virtual torque (VT) $P = M\omega_L$.

Therefore, instantaneous active and reactive powers are described by:

$$P = \frac{3}{2}\mathrm{Im}\left\{\mathbf{\Psi}_L^*\mathbf{I}_L\right\}\omega_L, \quad (13) \qquad Q = \frac{3}{2}\mathrm{Re}\left\{\mathbf{\Psi}_L^*\mathbf{I}_L\right\}\omega_L \qquad (14)$$

Based on eq. (12) can be written that:

$$P_{LSC} = \frac{3}{2}\omega_L\left(\Psi_{Lx}I_{Ly} - \Psi_{Ly}I_{Lx}\right) = \frac{3}{2}\omega_L\Psi_{Lx}I_{Ly} \qquad (15)$$

On the generator side electromagnetic power of the motor is defined by $P_e = M_e\Omega_m$. However, for calculation power of a generator side power losses should be taken into account: $P_{GSC} = P_e + P_{losses}$.

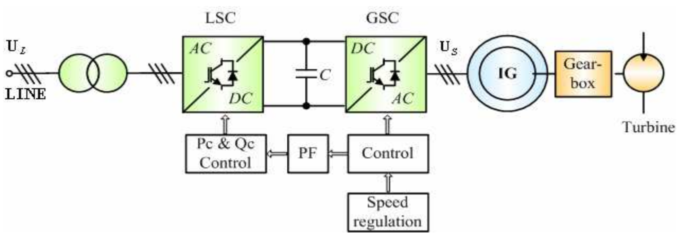


Fig. 10 Simplified configuration of the AC/DC/AC converter with control between generator and line

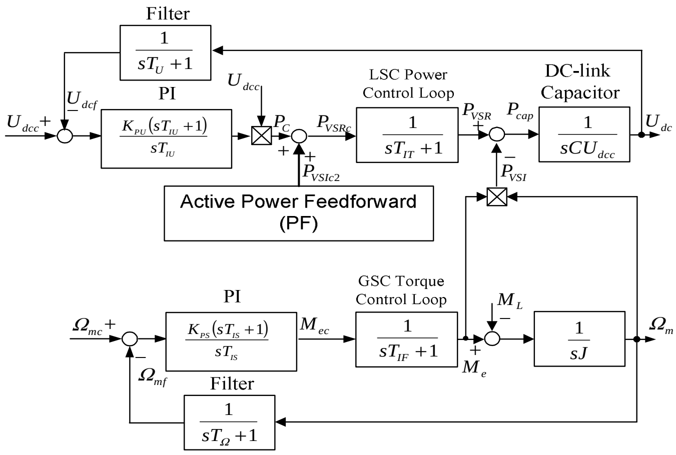


Fig. 11 Block diagram of the AC/DC/AC converter connected between generator and line with PF

Further, please consider a situation at stand still $(\Omega_m = 0)$ when nominal torque is applied. In such a case the electromagnetic power will be zero but the power delivered to the machine $P_{GSC}$ would have a significant value.

Estimation of this power is quite difficult, because the parameters of the machine and power switches are needed. Hence, for simplicity of the control structure a power estimator based on command stator voltage $\mathbf{U}_{Sc}$ and actual stator current $\mathbf{I}_S$ would be taken into consideration:

$$P_{LSC} = \frac{3}{2}\left(I_{Sx}U_{Sxc} + I_{Sy}U_{Syc}\right) \qquad (16)$$

### 3.3.1 Power Response Time Constants

Based on eq. (10) the time constant of the LSC powers control loop $T_{IT}$ is determined. With assumption that power losses of the converters can be neglected, power tracking performance can be expressed by:

$$P_{LSC}(s) = \frac{1}{1 + sT_{IT}}P_{LSCc}, \qquad P_{GSC}(s) = \frac{1}{1 + sT_{IF}}P_{GSCc} \qquad (17)$$

Where, $T_{IF}$ is the equivalent time constant of the GSC torque control loop. Based on this eq. (17) and assumptions described in [3] the analytic model of the AC/DC/AC converter between gen. and line with PF can be defined as in Fig. 11. Where, $T_U$, $T_\Omega$ filter time constants on actual DC-link voltage, and mechanical speed measurement; $K_{PU}, T_{IU}$; $K_{PS}, T_{IS}$ - PI dc voltage and speed controllers parameters. Moreover, it should be stressed that the first order filter added to DC-link voltage feedback strongly delays the signal.

## 4 Experimental Results

Proposed approach has been tested using Matlab and Saber simulator. Experimental investigation was conducted on a laboratory setup presented in Fig. 12. The setup consists of: input inductance, two PWM converter (VLT5005, serially

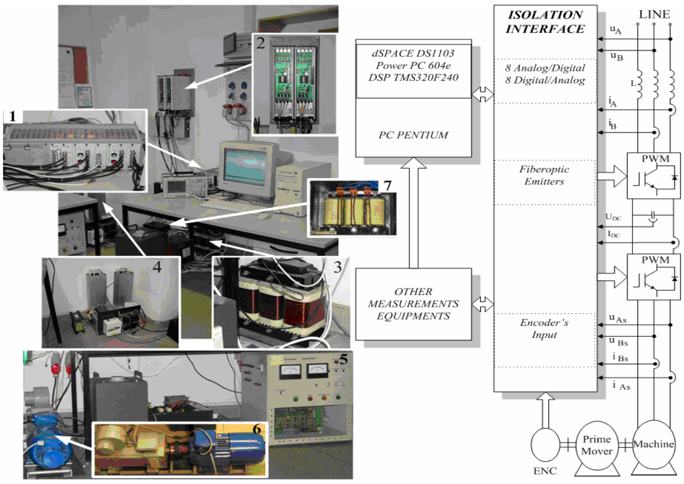

Fig. 12 Pictures and scheme of the laboratory setup, 1–isolating interface, 2- AC/DC/AC converter constructed based on two VSIs (Danfoss VLT 5005 with replaced control boards), 3– isolating transformer, 4– resistive load, 5– reversible rectifier, 6– machine set, 7– input choke

produced by Danfoss with replaced control interfaces) controlled by dSPACE DS1103 and induction machine with prime mover. The computer is used for software development and process visualization.

From Fig. 13 can be seen that steady states of the LSC provide sinusoidal like line current. Reactive power has a value close to zero. In further investigation, let check the quality of the PF during speed reversal. From Fig. 14b it can be seen that with PF result is superior in respect to DC-link voltage feedback only.

## 4 Conclusion

The paper shows that DPTC-SVM with active power feedforward assures stable and robust condition in steady state as well as in transients. Presented approach guarantee well line

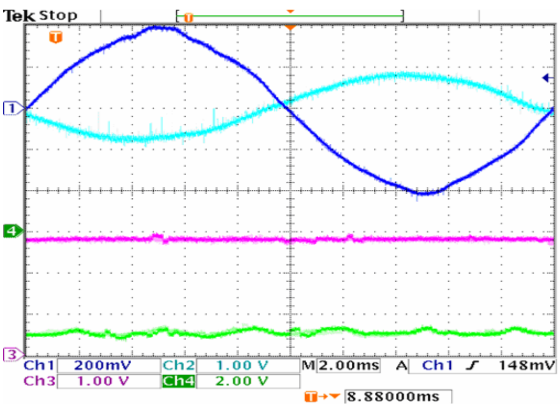

Fig. 13 Experimental steady state operation of LSC . a) prime mower torque -80% of nominal, mechanical speed 110% of nominal speed.

From the top: 1) line voltage 100V/div, 2) line current 10A/div, 3) DC-link voltage 200V/div and 4) line active power 1kW/div

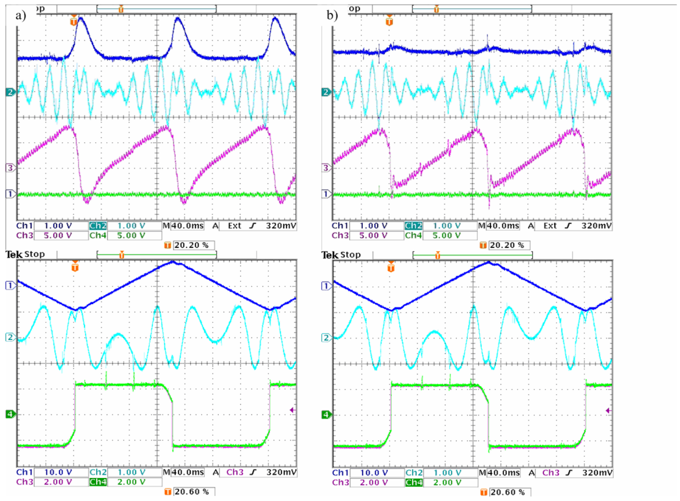

Fig. 14 Experimental speed reversal from 71% to -71% of nominal speed; a) Only DC-link voltage feedback b) With active power feedforward.

From the top: DC-link voltage 100V/div, line current 10A/div, active 2.5kW/div and reactive 2.5kVar/div power, mechanical speed of machine 1000rpm/div, stator current 10A/div, command and estimated torque 20 Nm/div. DC-link capacitor C=470uF

side power quality (THD <5%), minimized energy storage in DC-link capacitor, controllable and stable DC-link voltage as well as active and reactive line power control in whole rage of the rated power. However, induction generator has some drawback (e.g. it needs gearbox) which indicates that permanent magnet synchronous generator would be superior for WD MW. However, further investigations are required. Therefore, other solutions should be investigated and analyzed.

## Acknowledgement

The authors gratefully acknowledge the financial support of European Union 6FP (Project acronym: Wave Dragon MW Con. no.: 019983) and also dr Jasinski would like to thank The Foundation of Polish Science (FNP) for the support.

*References:*

[1] Web side: *www.wavedragon.net*

[2] H. Hur, at. al., "A Fast Dynamics DC-link Power-Balancing Scheme for a PWM Converter-Inverter System", *IEEE TIE*, vol. 48, No. 4, 2001, pp. 794–803,

[3] M. Jasinski, *Direct Power and Torque Control of AC/DC/AC Converter-Fed Induction Motor Drives*, Warsaw University of Technology, Ph.D. Thesis, Warsaw, Poland, 2005

[4] L. Christiansen, at. al., " Worlds Larges Wave Energy Project 2007 in Wales", *PowerGen 2006*,

[5] P. Vas, *Sensorless Vector and Direct Torque Control*, Oxford University Press,

[6] M. Zelechowski, *Space Vector Modulated-Direct Torque Controlled (DTC-SVM) Inverter-Fed Induction Motor Drive*, Warsaw University of Technology, Ph.D. Thesis, Warsaw, Poland, 2005